RGNZ/MGPB

Rudarsko-geološko-naftni zbornik
(The Mining-Geology-Petroleum Engineering Bulletin)
DOI: 10.17794/rgn.2026.5.2

Original scientific paper

Prediction of Mineral Reserves by a combination of Geophysical and drilling data using the Regression, Cokriging, and Artificial Neural network in the Mesgaran Copper Deposit, Iran

Kamran Mostafaei[1]*, Hamidreza Ramazi[2], Mohammad Zamani Ahmad Mahmoudi[3], Mitra Khalilidermani[3], Dariusz Knez[3]

[1] *Department of Mining, Faculty of Engineering, University of Kurdistan, Sanandaj, Iran.*
[2] *Faculty of Mining, Amirkabir University of Technology, Tehran, Iran.*
[3] *Department of Drilling and Geo-engineering, Faculty of Drilling, Oil and Gas, AGH University of Science and Technology, Krakow, Poland.*

Abstract

During a feasibility study of a mining project, a predictive model must be established to evaluate the profitability of the mineral deposit. In this research, three models were established by integrating geophysical data including Induced Polarization (IP) and Electrical Resistivity Tomography (ERT) with drilling data using the regression, Cokriging, and ANN techniques to determine whether the mineral production in the Mesgaran copper deposit is profitable or not. The Mesgaran deposit is located in the central part of the South Khorasan Province, Iran. The chargeability (*M*) and electrical resistivity (*ER*) data were used as input parameters, with copper grade as the output variable. The results of those predictive models were compared with an actual model obtained from twelve boreholes drilled after the feasibility study phase. Based on the conducted analyses, IP(*M*) data were found to be more suitable than *ER* data for constructing the 3D economic model of the copper deposit.. In addition, all three predictive models estimated the mean copper grade nearly equal to 0.15%. Nevertheless, a significant discrepancy was revealed in their predicted tonnage and profit values for the deposit. Overall, we conclude that the ANN algorithm provides more accurate and reliable estimates for mineral resource evaluation. The results of this research can be successfully utilized in the financial analysis of mining projects.

Keywords:
Reserve Estimation; Induced Polarization (IP); Artificial Neural Network (ANN); Geostatistics

1. Introduction

To explore and define economic mineral reserves, various investigative operations are employed. These operations include the excavation of shallow trenches, drilling and coring boreholes, the conducting of geophysical surveys, etc. After the implementation of the exploratory activities, the recorded data is used for reserve modelling of the studied deposit. Such models, known as block models, contain thousands of cubic-shaped blocks that represent the 3D shape of the deposit. In the block models, each block is specified by tonnage and mineral grade. The construction of such a 3D block model is an integral part of the exploration process of any profitable mineral reserve (**Mostafaei and Ramazi, 2018a, b**). Among the available exploratory methods, the geophysical techniques have acquired significant popularity since they are affordable, labourless, and time-effective. Every geophysical technique measures specific property subsurface formations to detect the rock type, mineral grade, density, electrical resistivity, porosity, etc. (e.g. **White et al., 2003; Reynolds 2011; Jodeiri et al., 2016**). Hence, depending on the deposit type, different geophysical techniques may be deployed for the subsurface characterization (e.g. **Mandal et al., 2013; Jodeiri et al., 2014; Mashhadi et al., 2017**). Regarding copper (Cu) deposits, usually two robust geophysical methods are applied: induced polarization (IP), and electrical resistivity tomography (ERT) (e.g. **Ferdows and Ramazi 2015; Biswas and Sharma, 2016; Mostafaei and Ramazi, 2019**). The use of 2D geophysical surveys in resource estimation is a cost-and tine-effective approach to constructing reliable 3D block models. The IP method is particularly effective in directly detecting sulfide minerals, which are the primary hosts of copper mineralization (e.g. chalcopyrite, chalcocite), as they exhibit a strong chargeability response. The ERT method, on the other hand, provides essential information on the host-rock structures and lithological boundaries. The combination of these two methods is therefore a powerful and widely used approach for exploring sulfide deposits, such as Volcanic Massive Sulfide (VMS)-type deposits, as it allows for both direct detection of mineralization and delineation of the geological setting.

In mining projects, geostatistical techniques are commonly adopted by mining engineers to perform resource

* Corresponding author: Kamran Mostafaei
e-mail address: k.mostafaei@uok.ac.ir, k.mostafaei@gmail.com
Received: 3 September 2025. Accepted: 3 March 2026.
Available online: 26 October 2026

estimation tasks (e.g. **Wang et al., 2010; Tutmez et al., 2007; Li et al., 2010; Shademan et al., 2013**). Geostatistical techniques are powerful tools to predict regionalized variables in space or time. These regionalized variables are obtained during the explorations operations, e.g. from common coring boreholes (**Mostafaei et al., 2014; Kumar et al., 2007**). The main geostatistical methods are kriging and cokriging. The basis of these techniques is to calculate a spatial model for the input data.

The calculation of variogram parameters requires adequate experience and engineering expertise in mining activities. Hence, the final variogram model is influenced by the engineer's skill and judgment. A wealth of valuable research has been conducted to process geophysical data using geostatistical techniques (e.g. **Park et al., 2011; Bourges et al., 2012; Azevedo and Soares, 2017; Salarian et al., 2020; Babaei et al., 2020**).

In recent decades, the applicability of the Artificial Neural Network (ANNs) in resource estimation tasks has been evaluated by several researchers (**Mostafaei et al., 2022a**). They reported that the main advantage of ANNs over statistical and geostatistical techniques is that the estimation task is conducted without making assumptions about the spatial variation of the mineral grade within deposits. The application of ANNs in resource estimation projects commenced in the early 1990s. During this decade, different researchers predicted the mineral grade in different ore bodies using ANNs (e.g. **Wu and Zhou, 1993; Galetakis, 1999; Singer and Kouda, 1996; Yama and Lineberrry, 1999**). Following those studies, **Ke (2002**) utilized ANNs to predict gold grade in a placer deposit located in Alaska, USA. In addition, **Koike et al. (2002); Koike and Mastuda (2003)** estimated the different mineral grades in the deposits situated in northern Japan. **Samanta et al. (2005)** applied the ANNs to predict the gold grade in the Nome placer deposit in Alaska, USA.

Moreover, the applicability of geostatistical techniques in resource estimation projects has been compared with ANNs. For instance, **Dutta et al. (2006)** predicted the Al_2O_3 and SiO_2 contents in an orebody using both kriging and ANNs. They concluded that both techniques provided similar predictions of Al_2O_3 grade; however, the SiO_2 grades predicted by the ANNs technique were more accurate. In similar research, **Misra et al. (2007)** utilized kriging and ANN techniques to estimate the arsenic grade in sediments of Circle City, Alaska, USA. They reported that the kriging technique delivered more reliable estimations than ANN. Additionally, ANNs have been successfully applied for geological horizon mapping in Croatia (**Šapina, 2016**), phosphate ore garade estimation in Egypt (**Embaby et al., 2023**), and the prediction of blast-induced flyrock in the Sungun copper mine, Iran (**Hanifehnia et al., 2024**).

The objective of this research is to establish an economical predictive model for the Mesgaran copper reserve. Here, an economic model refers to a block model that estimates the mineable resource, defined as the tonnage of material exceeding a specific cut-off grade that would be viable for extraction. Such a model is represented as a 3D block model in which each block possesses a specific grade and tonnage. The tonnage of each block is calculated based on its predefined volume (5*5*5m) and an assumed average rock density for the deposit. The data obtained from the IP and ERT surveys together with data from five coring boreholes were utilized as input data. Then the copper grade was estimated in all blocks through different techniques including regression, cokriging, and ANN models. The results of these techniques were compared with each other, and with the actual block model. The actual block model was generated using all boreholes drilled several months after the geophysical surveys. The research revealed that the ANN algorithm delivers a more reliable predictive model compared with the cokriging and regression models.

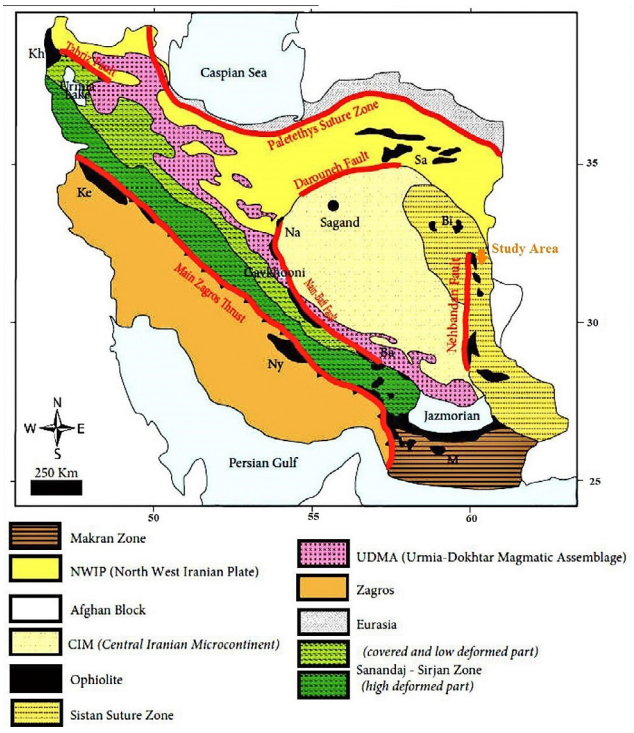


Figure 1: Location of the study area (Mesgaran copper deposit) on a map of the structural zones of Iran

1.1. Project description

The Mesgaran copper deposit is situated approximately 100 km from Birjand, the center of South Khorasan Province, Iran (see **Figure 1**). The name of the deposit originates from the adjacent Mesgaran Village (see **Figure 2**).

Figure 1 displays a map of the structural zones of Iran, with the location of the Mesgaran copper deposit highlighted as the case study area. Geologically, the deposit lies within the Sistan Suture Zone. The Sistan Suture Zone contains two primary subzones: Flysch, and

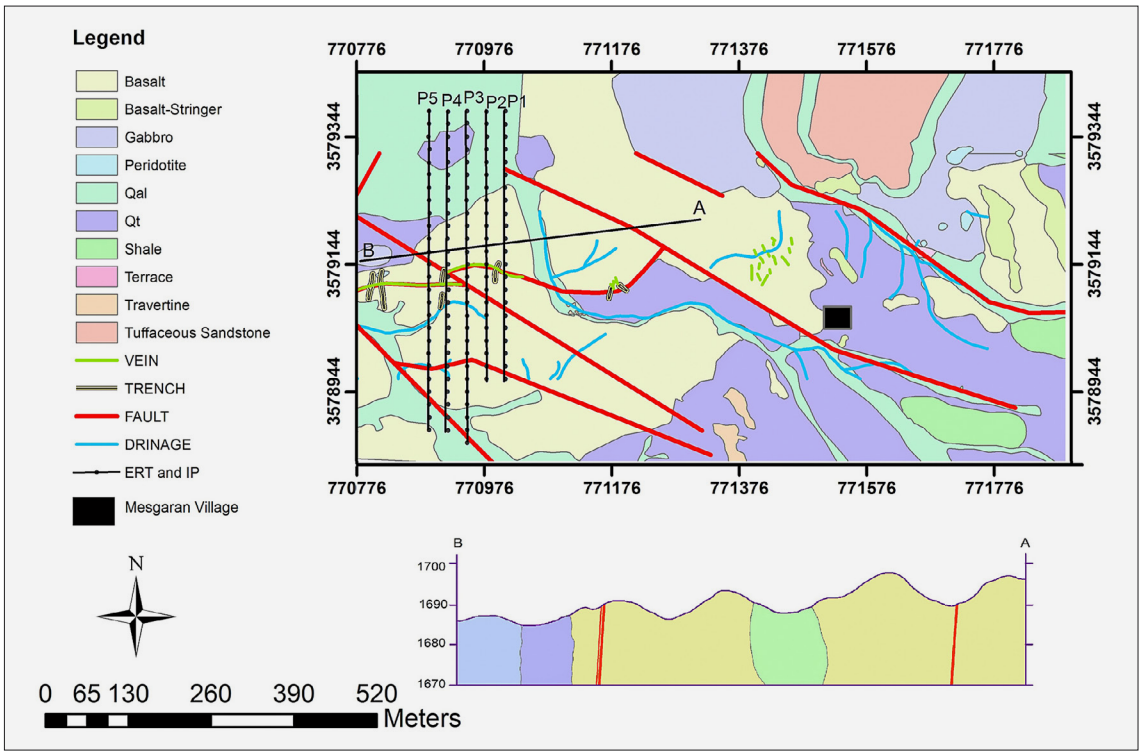


Figure 2: The lithological units along with the array of geophysical profiles in the study area

Lut block. The study area falls in the Flysch subzone which remarkably hosts the tectonized terrains composed of thick sediments, (e.g. shale and limestone) and igneous rocks such as basalt and rhyolite.

The main lithology of the Mesgaran copper deposit encompasses the massive basaltic and ultrabasic formations. The distribution of the different lithological structures in the deposit has been depicted in **Figure 2**. Based on the field geological mapping the local mineralization trend is in the direction NW-SE. As shown in this figure, the IP and ERT surveys were performed through five sections, i.e. P1, P2, P3, P4, and P5.

The age of the lithological units dates back to the Cretaceous period, although in some spots, Quaternary sediments are also present. The dominant types of local alterations are chlorite and serpentine. More importantly, the deposit is a volcanic massive sulfide (VMS) deposit. In addition, chalcocite and chalcopyrite are the primary copper minerals in the deposit.

2. Methods

2.1. Geophysical Methods: Electrical Resistivity Tomography(ERT) and Induced Polarization (IP)

In mineral exploration, geophysical methods are considered the primary, most important, and diverse techniques (**Mostafaei and Kianpour, 2022b**). The ERT technique is one of the most widespread geophysical methods used in exploration activities. The basis of this technique is to utilize direct current (DC) resistivity to characterize the subsurface rocks. In other words, electrical resistivity is the key factor in differentiating formations based on the change in some geological and hydrogeological characteristics of the subsurface rocks (e.g. **White et al., 2003; Loke and Barker 1996a; Loke and Barker 1996b**). In this method, direct current is injected into the ground through two current electrodes, and the resulting electric potential is measured between two separate potential electrodes. The electric current is transmitted to the subsurface rocks, and then, it is received via electronic conduction (**Reynolds, 2011**). ERT is an advanced geophysical technique designed to image the subsurface in two or three dimensions by measuring its electrical resistivity. It employs a multi-electrode array to inject direct current into the ground and measure the resulting potential differences at numerous locations. Through the inversion of a large number of these apparent resistivity measurements, the method produces a quantitative model of the true resistivity distribution, which can be interpreted to delineate geological structures, lithological variations, and fluid content (e.g. **Reynolds, 2011; Stanley and Bolton, 2008**). Through the measured electrical resistivity, a number of properties of the rocks can be estimated. Such properties include the porosity, rock type, pore fluid, and mineral composition. Those properties are then used to build the 3D model of the subsurface strata (**Mostafaei and Ramazi, 2018b**).

The IP technique is a powerful tool to recognize and classify underground rock layers. This method has been

applied in resource estimation tasks since the 1950s. The basis of the time domain IP techniques is to inject current into the ground and, after its measure the resulting transient voltage (secondary field). These measurements are then inverted to produce a 2D/3D model of subsurface chargeability. The IP surveys are conducted either in the frequency or time domain (**Fink et al., 1990**). Regarding the frequency domain, the apparent resistivity is recorded through several frequencies which are commonly less than 10 Hz (**Khesin et al., 1997**). In this research, the time domain was applied, the decay voltage between two potential electrodes, is recorded as a function of time. This is stated as the parameter of apparent changeability (**Everett, 2013**):

$$M = \frac{1}{V_C} \int_{t_1}^{t_2} V(t)dt \quad (1)$$

Where *M* represents the apparent chargeability (msec), *V_C* is the potential voltage (volt), *t* is time (sec), and *V(t)* is the potential voltage function. **Equation 1** can be written as **Equation 2** (**Everett, 2013**):

$$M = \frac{1}{V_0[t_{i+1} - t_i]} \int_{t_i}^{t_{i+1}} V(t)dt \quad (2)$$

Both IP and ERT surveys can be conducted through the common arrays of Wenner, Schlumberger, pole-dipole, and dipole-dipole. The latter array has been utilized in this research. It is less sensitive to the vertical variation of electrical resistivity. However, such sensitivity is significant in the horizontal direction (**Dahlin et al., 2002; White et al., 2003**).

2.2. Regression analysis

Regression analysis is a powerful statistical tool widely used in geoscience to determine unknown parameters by extracting mathematical correlations between geological variables (**Howarth, 2001**). In this research, it was employed not merely as a statistical tool, but as a core interpolation method to estimate copper grade across the entire deposit. The primary goal was to derive a continuous mathematical function that best describes the relationship between the geophysical attributes (*M*&*ER*) and the copper grade obtained from drill holes, recognizing the influence of each independent variable on the output (**Khanlari et al., 2012**).

While various types of regression exist (e.g. linear, logistic, and polynomial), a polynomial regression was selected for this study. This choice was driven by its significant capability to approximate complex, non-linear relationships, which are common in geological data, as opposed to the often-imprecise correlations provided by linear regression.

The applicability of the polynomial regression is significant since miscellaneous mathematical functions can be approximated as polynomial relations (**Howarth, 2001**). The general form of the extracted polynomial correlation is:

$$y = B0 + B1x + B2x^2 + ... + Bn\,x^n \quad (3)$$

where y stands for the dependent variable, x indicates the independent variable, and *B0, B1,… Bn* are constants.

The analysis was performed on the composited dataset. The optimal polynomial degree was selected by evaluating the coefficient of determination (R^2). This approach of using a derived regression function for spatial prediction is well-established in geoscience, as demonstrated in similar resource estimation studies (e.g. **Malvić et al., 2025**). The resulting function with the highest R^2 value was then applied as an interpolation method to the 3D block model of the deposit. Each block's geophysical attribute (*M* or *ER*) was used as input (x) into the derived polynomial equation to predict and assign a copper grade value (y) to that specific block, thereby achieving a continuous interpolation of grade across the entire volume.

2.3. Cokriging estimator

Geostatistical methods employ statistical techniques to estimate the spatial correlations between the geological variables in 3D space. They consider key spatial parameters, including the distance and direction between sample points, in their calculations. The distance and direction are mathematically incorporated into the variogram tool. Due to this rigorous approach, resource estimation performed using geostatistical methods typically achieves a lower estimation error compared to many other available (**Knotters et al., 1995**).

The cokriging estimator is a poweful geostatistical technique for estimating unknown variables, e.g. mineral grade, in explored deposits. As a matter of fact, it is a generalized form of the multivariate and univariate linear regression models which are capable of estimating the grade at different spots, planes, and 3D shapes. The mathematical foundation of cokriging relies on modelling the sapatial auto-correlation of variables through variograms and their cross-correlation through cross-variograms (**Malvić et al., 2009**). The experimental variogram for a regionalized variable Z at lag distance h is calculated as:

$$\gamma(h) = \\ = (1/(2N(h))) \times \Sigma_{i=1}^{N(h)} [Z(x_i) - Z(x_i + h)]^2 \quad (4)$$

where *N(h)* is the number of data pairs separated by lag *h*. for cokriging, the cross-variogram between primary variable Z_1 and secondary variable Z_2 is defined as:

$$\gamma_{12}(h) = (1/(2N(h))) \times \Sigma_{i=1}^{N(h)} [Z_1(x_i) - Z_1(x_i + h)] \times \\ \times [Z_2(x_i) - Z_2(x_i + h)] \quad (5)$$

These experimental variograms are fitted with theorical models such as spherical, exponential, pre gaussian

models (**Salarian et al., 2024**). These spherical models, for instance, are expressed as:

$$\gamma(h) = \begin{cases} c_0 + c \times [(3h)/(2a) - (1/2) \times (h/a)^3] & if\ h \le a \\ c_0 + c & if\ h > a \end{cases} \quad (6)$$

Where C_0 is the nugget effect, C is the partial sill, and a is range parameter.

In the cokriging estimator, a certain parameter is set as the primary variable while one or several other parameters are defined as the secondary variables. The cokriging technique includes the simple kriging estimator which uses the data of such correlated secondary variables (**Hooshmand et al., 2011**). The cokriging estimator at an unsampled location X0 is given by the linear combination:

$$Z_1^*(x_0) = \Sigma_{i=1}^{n1} \lambda_i Z_1(x_i) + \Sigma_{j=1}^{n2} \omega_j Z_2(x_j) \quad (7)$$

where λ_i and ω_j are the weights determined by solving the cokriging system that minimizes the estimation variance while ensuring unbiasedness.

A key characteristic of the cokriging estimator is its incorporation of the covariance between the regionalized variables. This technique offers that the cokriging technique exhibits high accuracy, especially if the primary variable is sparse, and the pertinent secondary data is available. The accuracy of the mineral grade estimation results can be enhanced if an auxiliary variable is used in the calculations. If the measurement of such auxiliary variables is affordable, the need for conduction of the expensive measurement of other variables reduces dramatically (**Boezio et al., 2011; Xu et al., 2015**).

2.4. ANN approach

The ANN approach functions based on the structure human neuron cells. Each neural network includes three main layers: the input, hidden, and output layers. Each layer contains a set of specific neurons that perform different tasks to finally produce accurate outputs (e.g. **Singh et al., 2013**). The mathematical operation of each neuron can be represented as:

$$y_j = f(\sum(w_ji \times x_i) + b_j) \quad (8)$$

Where *X*i are the input values, *W*ji are the connection weights, *bj* is the bias term, and *f* is the activation function (**Šapina, 2016**; **Embaby et al., 2023**).

The ANN model receives one or more geological attributes as the input variables, and after training, it estimates the mineral grade as the output variable. The training process involves minimizing the mean squared error (MSE) between the predicted and actual values:

$$MSE = (1/N) \times \sum(y_predicted - y_actual)^2 \quad (9)$$

In this study, we employed the Levenberg-Marquardt optimization algorithm for network training, which has demonstrated high efficiency in similar geoscientific applications (e.g. **Hanifehnia et al., 2024; Nguyen et al., 2023**).

In the training phase, spatial relations between the input and output variables are recognized without the need for explicit "interval" or "variogram" calculations based on deposit structure. Furthermore, the ANN approach, can remove noise from the data, thereby leading to more accurate mineral grade prediction. Since in most economic ore bodies, the mineralization distribution is highly complex, the ANNs can effectively estimate the reserve profitability during the feasibility studies (e.g. **Yama and Lineberrry, 1999; Mostafaei et al., 2022a; Mostafaei et al., 2023**). This capability is particularly valuable in complex mineralization patterns where traditional geostatistical methods may struggle to capture inherent spatial relationships, as demonstrated in various mineral deposit types (e.g. **Šapina, 2016; Embaby et al., 2023**).

3. Results

3.1. IP and ERT inversion modelling

According to the topography and geological setting, the dipole-dipole array was selected for the surveys. Five parallel profiles were established with a spacing of 30m along a N-S azimuth. For this array, an electrode spacing (a-spacing) of 20 m was used, and the n factor (the separation factor or jump between the current and potential dipoles) was varied from 1 to 10 to achieve different investigation depths. The quality of the acquired ERT and IP data was generally good, as evidenced by the smooth inversion models and low root-mean-square (RMS) errors. The inversion process yield RMS errors typically below 10% for the ERT data and below 5% for the IP data, ensuring reliable imaging of subsurface. A number of 1000 data points were measured, and then they were corrected, and inverted using the 2D numerical modelling in Res2dinv software. It is worth mentioning that the Newton and Gauss-Newton approaches were applied for this purpose. In what follows, the results obtained from the 2D inversion modelling of all profiles are elaborated.

Profile 1 (P1)*:* This profile was situated in the eastern segment of the study area and was 350 m in length. **Figure 3** depicts the corresponding results obtained from the inverse modelling. The maximum values of the chargeability *(M*), and electrical resistivity (*ER*), were calculated as 60 msec and 360 Ωm, respectively. Two anomalies were detected along this profile: A1 and A2 (see **Figure 3**). The A1 anomaly is located at 160 – 180 m along the profile. Moreover, its top at a depth of 35 m in which the chargeability varies between 40 – 60 msec, and the electrical resistivity changes in the range of 175 - 300 Ωm. The A2 anomaly lies between 50 and 60 m along the profile. Furthermore, the chargeability fluctuates between 50 and 60 msec, and the electrical resistivity varies from 200 – 250 Ωm.

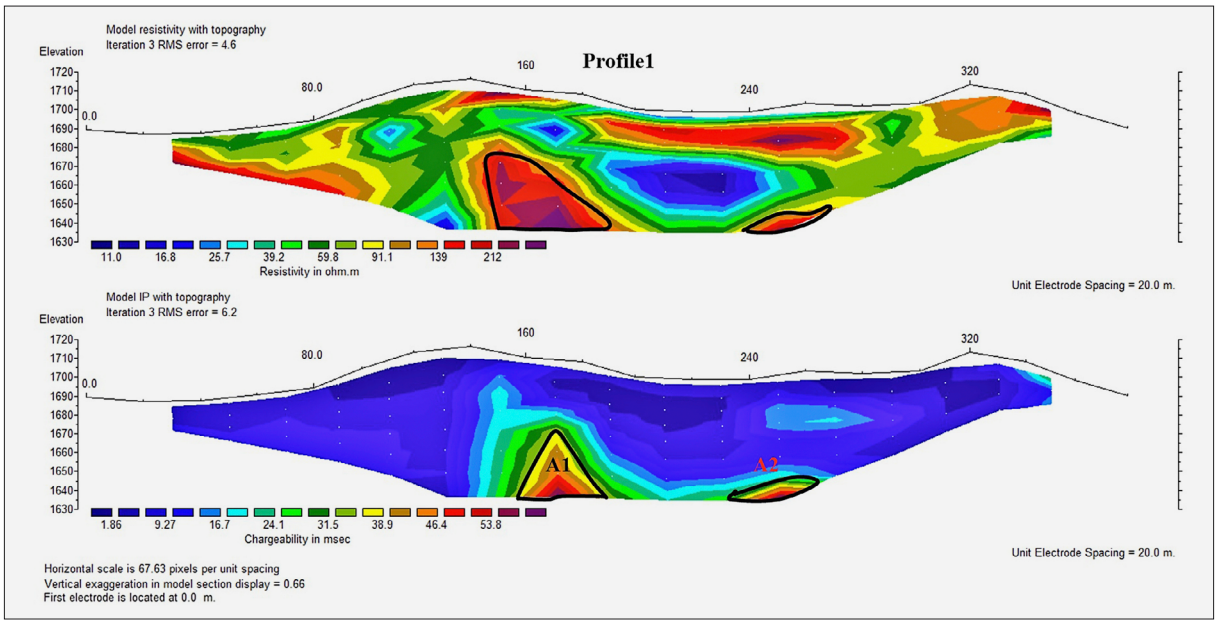


Figure 3: The electrical resistivity and IP (chargeability) sections obtained from profile 1

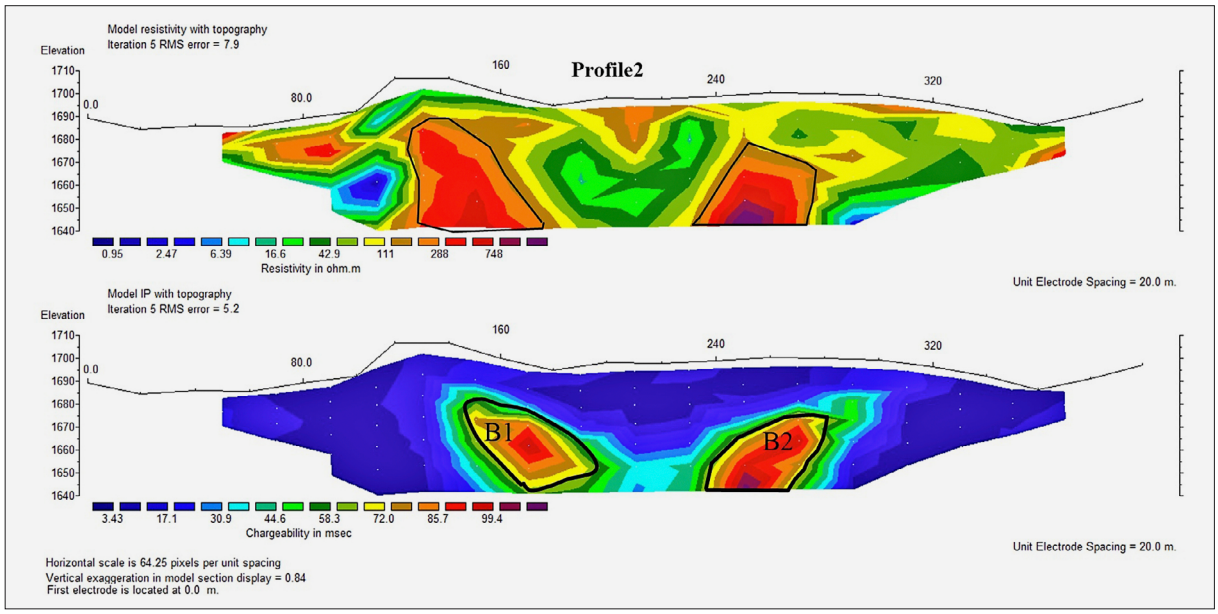


Figure 4: The electrical resistivity and IP (chargeability) sections obtained from profile 2

Profile 2 (P2): This profile was 400 m in length. **Figure 4** illustrates the pertinent results achieved from the inverse modelling. There were two anomalies detected in this profile: B1 and B2. The B1 anomaly starts from a depth of 30 m and stretches towards the depth of 50 m. The chargeability varied between 50 – 85 msec, and the electrical resistivity changed in the range of 300 - 700 Ωm. Regarding the B2 anomaly, it is located 250 m far from the beginning of the profile. Moreover, its depth varies from 30 to 60 m. The maximum value of the chargeability is 110 msec, and the maximum of electrical resistivity is equal to 2200 Ωm. In term of economic potential, the B2 anomaly is more significant (or valuable) than B1.

Profile 3 (P3)*:* This profile was 520 m in length. **Figure 5** shows the corresponding results achieved from the inverse modelling. The maximum value of the chargeability is 110 msec, and the maximum electrical resistivity is 1160 Ωm. A number of three anomalies were detected through this profile: C1, C2, and C3. The C1 anomaly is at the distance 250 m from the beginning of the profile, and its depth varies from 45 m to 65 m. The corresponding chargeability is between 65 to 90 msec, and the electrical resistivity varies from 350 to 1150 Ωm. Regarding the C2 anomaly, it is located at the end of the profile. The corresponding apparent chargeability amounts to 110 msec, and the resistivity is around 300 Ωm. The C3 is a shallow anomaly with a depth of 15 m.

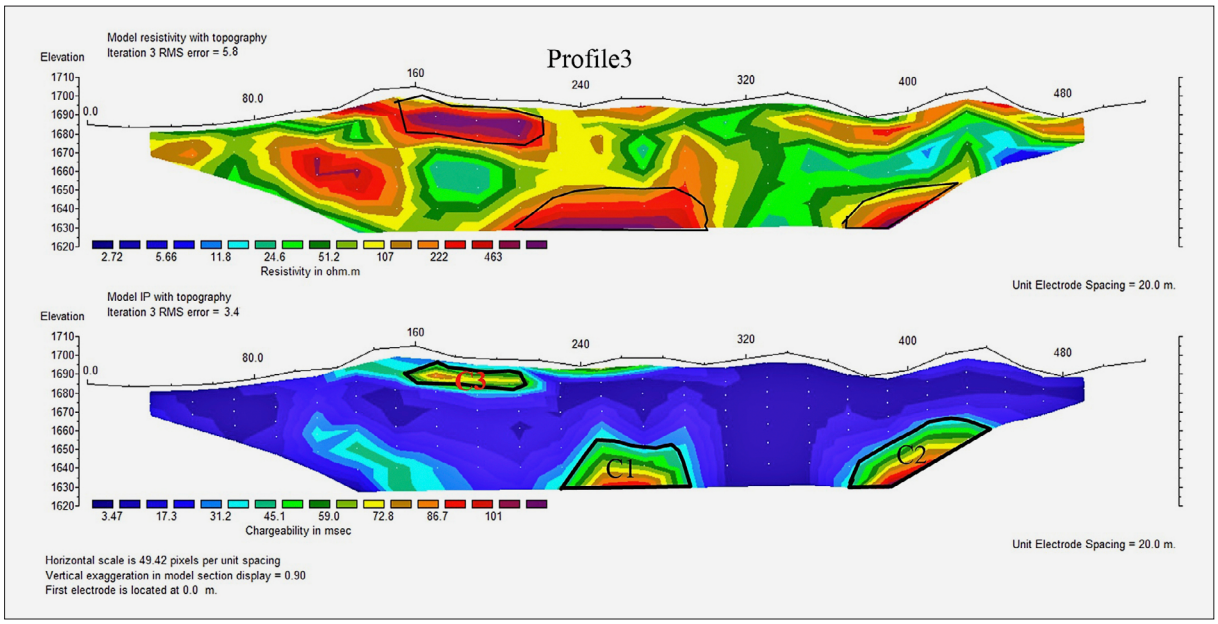


Figure 5: The electrical resistivity and IP (chargeability) sections obtained from profile 3

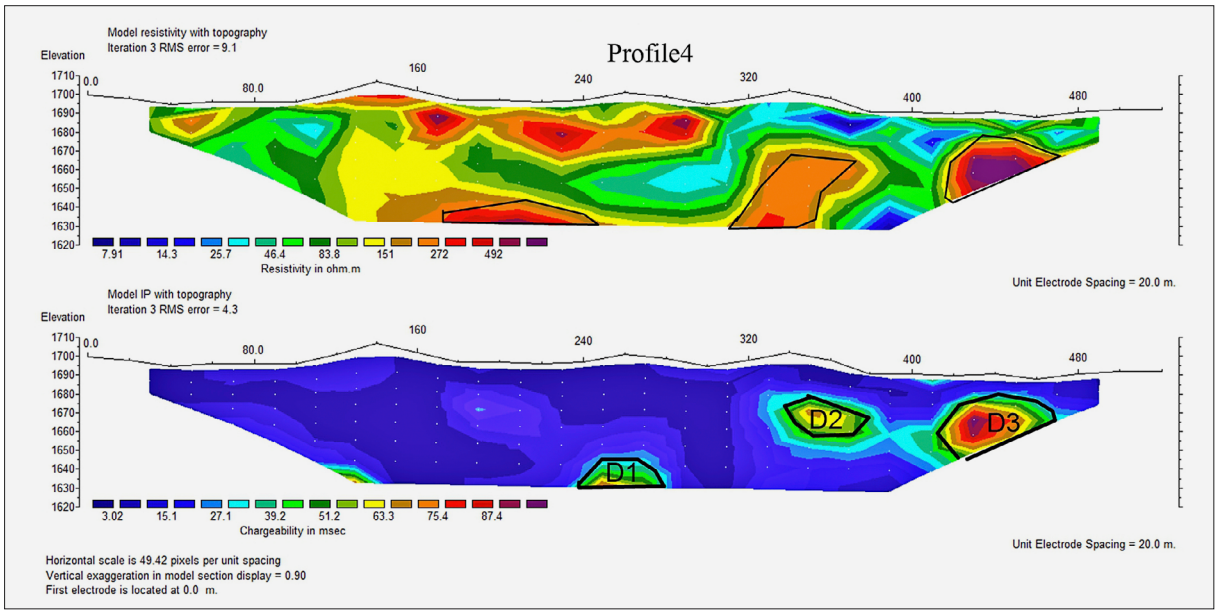


Figure 6: The electrical resistivity and IP (chargeability) sections obtained from profile 4

The pertinent chargeability varies from 60 to 90 msec, and the electrical resistivity amounts to 300 Ωm.

Profile 4 (P4): This profile was 520 m in length**. Figure 6** illustrates the pertinent results achieved from the inverse modelling. Three anomalies were detected in this profile: D1, D2, and D3. The maximum value of the chargeability was 100 msec, and the maximum values of electrical resistivity was equal to 600 Ωm. The D1 anomaly is located 240 m far from the beginning of the profile, and its depth amounts to 60 m. The corresponding chargeability varies from 50 msec to 70 msec, and the electrical resistivity changes in the range of 300 - 500 Ωm. Regarding the D2 anomaly, it is located 360 m far from the beginning of the profile. Moreover, it lies between the depths of 15– 35 m. The pertinent value of the chargeability varies between 30 - 60 msec, and the electrical resistivity is between 150 - 300 Ωm. The D3 is a surface anomaly with a depth ranging from 10 m to 45 m. The pertinent chargeability amounts to 90 msec, and the electrical resistivity reaches 1000 Ωm.

Profile 5 (P5): This profile was 350 m in length. **Figure 7** shows the pertinent results obtained from the inverse modelling. There are two anomalies detected via this profile: E1, and E2. In this profile, the intensity of mineralization is less than in the previous profiles. The maximum value of the chargeability is 85 msec, and the maximum value of electrical resistivity is 750 Ωm. The E1 anomaly is located 160 m from the beginning of the

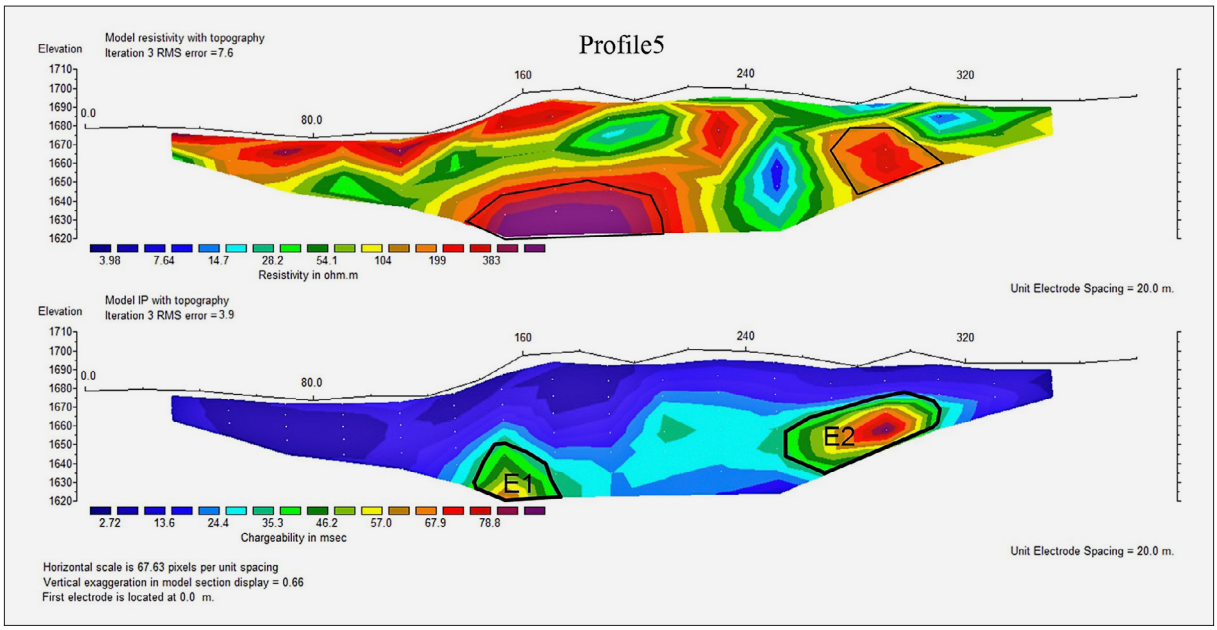


Figure 7: The electrical resistivity and IP (chargeability) sections were obtained from profile 5

profile, and its depth amounts to 55 m. The corresponding chargeability varies between 40– 60 msec, and the electrical resistivity changes in the range of 200 - 700 Ωm. Regarding the E2 anomaly, it is located 270 m from the beginning of the profile. In addition, it lies between the depths of 25– 45 m. The pertinent value of the chargeability is between 40 - 80 msec, and the electrical resistivity varies from 300 to 400 Ωm.

In the aforementioned paragraphs, the inversion modelling results of all profiles were concisely presented. The results exhibit a direct correlation between the *M* and *ER* data in the deposit. The deposit has remarkable values of chargeability and electrical resistivity. The measured chargeability across the deposit varies from background levels of less than 5 to values exceeding 110 msec in most prominent anomalies. Similarly, electrical resistivity ranges from around 10 to over than 2000 Ωm.. Overall, the results demonstrate that the mineralization phenomenon mainly occurred in the veins and lenses parallel to the E-W direction. As mentioned in section (2), the Mesgaran copper deposit is a massive volcanic sulfide in which the copper mineralization occurred within the faults. Hence, the copper zones are the locations with significant values of chargeability and electrical resistivity.

3.2. Detection of copper mineralization zones

To detect the copper mineralization zones in the Mesgaran deposit, firstly, a 3D block model was generated using the inverted data of chargeability, *M*, and electrical resistivity, *ER*, via the Datamine Studio software. The size of all blocks was 5m × 5m × 5m. Then, the *M* and *ER* values were estimated for all blocks using the Kriging method. The variography was done using the SGeMS software. Hence, experimental variogram were calculated for different spatial directions (azimuths) and vertical distance. These were then used to fit theoretical variogram models and derive their parameters (sill, range, nugget effect). **Figure 8** depicts the generated block model. Regarding the *M* and *ER* values, three different classes were defined. The corresponding classes are shown in **Table 1**.

Based on the above classification, the blocks with high values of *M* and *ER* were filtered. Two copper mineralization zones were detected in the deposit. The first one was situated in the middle of the deposit with the strike parallel to the E-W direction, in the depth range of 40 m – 60 m. The second zone was detected in the southern part of the deposit. The latter zone was smaller than the first one. Both zones are of paramount importance from the perspective of mining profitability.

3.3. Resource estimation

In this research, the resource estimation was carried out in a creative manner. The chargeability and electrical resistivity data obtained from the inverse modelling were separately utilized as the input data. Furthermore, the Cu_{grade} data obtained from a number of five coring boreholes was also prepared. Through this, a dataset containing the *M*, *ER*, and Cu_{grade} was created. To array the data in regular depth intervals, the composition process was done for the dataset. The interval depth was set equal to 5 m. In **Table 2**, the statistical parameters related to the *M*, *ER*, and Cu_{grade} in the composited dataset have been summarized.

The composited dataset was then applied in the regression analysis, Cokriging estimator, and ANN model to find the correlation between the *M* - Cu_{grade} and *ER* -

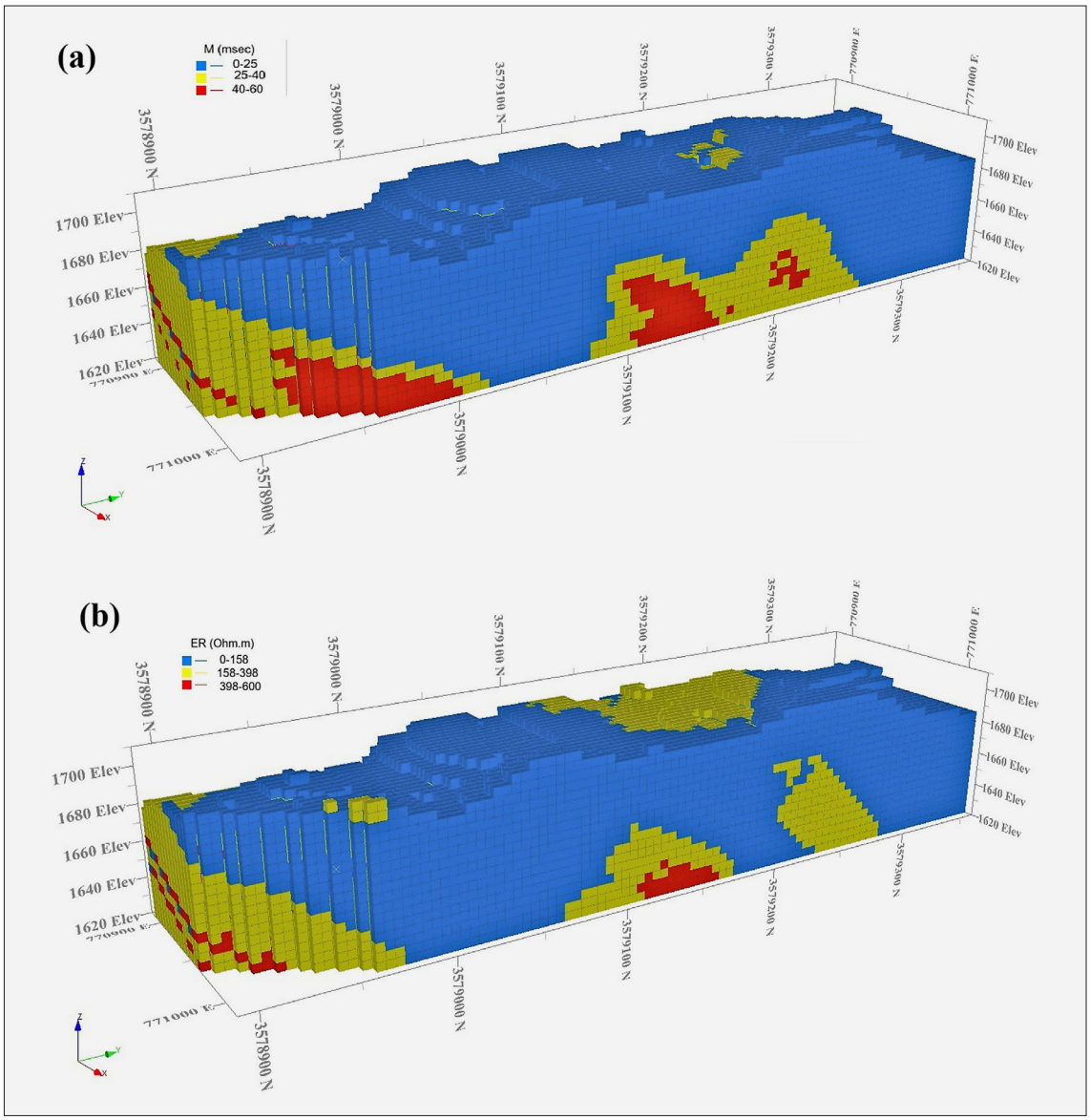


Figure 8: The 3D block models generated for (a) IP model as *M*; and (b) electrical resistivity as *ER* in the Mesgaran copper deposit.

Table 1: Classification of estimated values of chargeability and resistivity in the block models.

Block attribute	Defined classes
M (msec)	Low: [0 – 25]
	Medium: [25 – 40]
	High: [40 – 60]
ER (Ωm)	Low: [0 – 158]
	Medium: [158 – 398]
	High: [398 – 600]

Cu_{grade} pairs. The pertinent results are described in the following subsections:

3.3.1. Regression analysis

To perform the regression analysis, initially, the correlation between the *M* and Cu_{grade} values, in the composited dataset, was extracted. The corresponding correlation is:

$$Cu_{grade} = (66 \times 10^{-4}) - (32 \times 10^{-4})\, M + \\ + (35 \times 10^{-5})M^2 - (1 \times 10^{-6})M^3 \qquad (10)$$

Table 2: The statistical parameters of the different variables in the composited dataset.

Parameter	Symbol	No. of samples	Max.	Ave.	Min.	Std. dev.
chargeability (msec)	*M*	80	100	16.8	1	19
Electrical resistivity (Ωm)	*ER*	80	1320	160.6	17	168
Cu grade (%)	Cu_{grade}	80	2.34	0.14	0.002	0.37

where, Cu_{grade} represents the copper grade (%), and M is the apparent chargeability (msec). The R-sq of the above correlation was 90%, thereby indicating the high fit of the extracted relationship.

In the next step, the correlation between the Cu_{grade} and ER, in the composited dataset, was extracted. The pertinent correlation is as:

$$Cu_{grade} = -(135 \times 10^{-3}) + \\ + (17 \times 10^{-4})ER - (1 \times 10^{-7})ER^2 \qquad (11)$$

Where, Cu_{grade} indicates the copper grade (%), and ER is the resistivity (Ωm). The R-sq of the above correlation was 51%, thereby representing less accuracy of the extracted relationship.

Since the accuracy of **Equation 10** is markedly significant, it was utilized to estimate the Cu_{grade} in all blocks. **Table 3** shows the corresponding results of economic resource estimation. Based on this table, the tonnage of the Mesgaran copper deposit was calculated as 185000 tons with an average of Cu_{grade} equal to 0.15%.

Table 3: Results of economic resource estimation using the regression analysis

Min Cu_{grade} (%)	Max Cu_{grade} (%)	Cutoff grade Cu_{grade} (%)	Mean Cu_{grade} (%)	Tonnage (ton)
0.002	2.7	0.05	0.15	185,000

3.3.2. Cokriging estimator

As it was mentioned in the previous section, the correlation between the Cu_{grade} and M data was found to be noticeably larger than the Cu_{grade} – ER pair. Therefore, the resource estimation was only conducted by incorporation of the chargeability data in the cokriging estimator. The cokriging estimator was composed of two main variables: the primary, and the secondary variable. In this research, firstly, the Cu_{grade} and M were set as the primary and secondary variables, respectively. Then, the variography of the Cu_{grade} – M data was performed. Afterwards, the corresponding cross-variogram was computed. The pertinent variogram parameters including the experimental model, sill, nugget, and rang are tabulated in **Table 4**.

Table 4: Variogram parameters in the cokriging estimator

Experimental semi-variogram	Fitted model	Sill	Rang	Nugget effect
IP(M)	Gaussian	450	45	45
Cu_{grade}	Gaussian	0.1	67	0
Cross- variogram	Gaussian	9.6	54	1.7

Based on the variogram parameters, the values of Cu_{grade} were estimated in all block models. It is noteworthy that the search radius was set as 40 m. Moreover, the minimum and maximum of the participating points in the grade estimation process were specified as 3 and 15. **Table 5** illustrates the obtained results of economic resource estimation through the cokriging estimator. Based on this data, the tonnage of the Mesgaran deposit was computed as 146000 tons with an average Cu_{grade} equal to 0.14%.

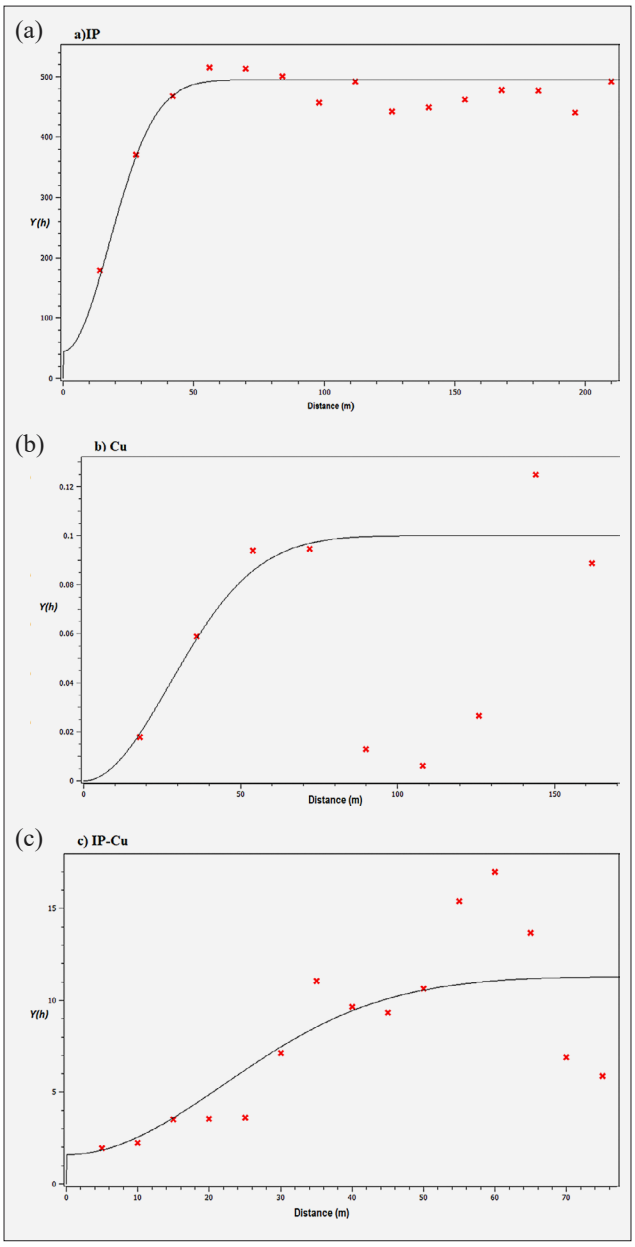


Figure 9: The experimental variogram models for (a) IP data (M); (b) Cu; and (c) cross-variogram of (M) and Cu

3.3.3. ANN model

The corresponding code of the ANN model was prepared, and run in the Matlab software setting. Similar to the cokriging model, the composited chargeability dataset was utilized as the input data. For this purpose, 70% of the IP records were set for the training of the ANN model while the rest of the data used for the testing phase. A number of several algorithms were examined

Table 5: Results of resource estimation using cokriging estimator

Min Cu_{grade} (%)	Max Cu_{grade} (%)	Cutoff grade Cu_{grade} (%)	Mean Cu_{grade} (%)	Tonnage (ton)
0.025	2.4	0.05	0.14	146,000

Table 6: Results of resource estimation using the ANN algorithm

Min Cu_{grade} (%)	Max Cu_{grade} (%)	Cutoff grade Cu_{grade} (%)	Mean Cu_{grade} (%)	Tonnage (ton)
0.012	2.5	0.05	0.16	170,000

for the training process, and ultimately, based on the acquired results, the Levenberg-Marquardt (LM) algorithm was selected. Moreover, the number of neurons in the hidden layers was adjusted from 2 to 20. After performing the algorithms, the optimal number of the neurons was obtained equal to 8.

Based on the prepared code, the Cu_{grade} was estimated in the entire deposit. **Table 6** shows the results of economic resource estimation through the created block model. As it can be observed, the tonnage of the deposit was forecasted equal to 170000 tons with average Cu_{grade} equal to 0.16%.

4. Discussion

The primary objective of this analysis is to assess the performance of different estimation techniques under the data-constrained conditions typical of an early-stage feasibility study. **Section 3.3.1**. revealed that correlating the chargeability data and Cu_{grade} values in the blocks is more appropriate. Therefore, the resource estimation was conducted by incorporating of the chargeability data to the regression model, cokriging estimator, and the ANN model. The corresponding results were summarized in **Table 3**, **Table 5** and **Table 6**.

Several months after the geophysical surveys were completed, seven supplementary coring boreholes were drilled. Consequently, a reference (actual) block model was created using all coring boreholes (12 boreholes). The copper grade values of all blocks were then estimated using the kriging technique on this reference block model. It is noteworthy that the input data used in the actual model was almost twice the data used in the regression estimations, cokriging, and ANN models. **Table 7** shows the resource estimation results obtained from the actual block model.

Thus, the prediction models generated by mentioned techniques (regression, ANN, and cokriging) using five boreholes data and *M&ER* data as auxiliary variables, were compared against a reference actual model built using assay data from all twelve available boreholes.

Comparing **Table 3**, **Table 5**, **Table 6**, and **Table 7**, it can be seen that the range (minimum and maximum) of

Table 7: Results of resource estimation using all boreholes data (actual block model)

Min Cu_{grade} (%)	Max Cu_{grade} (%)	Cutoff grade Cu_{grade} (%)	Mean Cu_{grade} (%)	Tonnage (ton)
0.010	2.5	0.05	0.15	160,000

Table 8: The error percentage of the different estimation methods compared to the actual block model

No.	Estimation method	Tonnage Estimation Error (%)
1	Regression	+15.63
2	Cokriging	-8.75
3	ANN	+6.25

Cu_{grade} values estimated by the regression model is wider than the cokriging estimator and ANN model. However, the mean the Cu_{grade} predicted by all techniques is very close to the actual value (0.15%). Furthermore, the cokriging technique underestimated both the ore tonnage and the economic value of the deposit while, the regression model overestimated them. In contrast, the ANN model predicted these parameters closer to the actual block model. Thus, it can be concluded that the ANN model provides more precise resource estimation results compared to the regression model and cokriging estimator.

Furthermore, to compare those three techniques, their estimation errors related to the tonnage, and economic value (profitability) were computed. To do this, the underlying formula was utilized for all three parameters:

$$Estimated\ error = \frac{Predicted\ Value - Actual\ Value}{Actual\ Value} \times 100 \quad (7)$$

Table 8 presents the corresponding results. The positive sign indicates overestimation while the negative sign indicates underestimation. As shown, the ANN and cokriging techniques yield lower tonnage estimation errors than the regression model. Consequently, the profitability predicted by the ANN and cokriging model is more accurate than that from the regression analysis. Comparing the performance of the ANN and cokriging techniques, it is evident that the results of the ANN model are more reliable. Furthermore, it should be noted that since the input data used in the ANN model and the cokriging estimator was half of the data used in the actual block model, the performance of these models is completely acceptable. These results corroborate the findings by **Dutta et al. (2006**). The corresponding ANN code will be utilized for the resource estimation task during the future development of the exploratory activities in the Mesgaran copper deposit.

5. Conclusions

This study assessed the reliability of three predictive approaches -regression analysis, cokriging and artificial

neural networks (ANN) for early-stage resource estimation under data-limited conditions. The evaluation strategy was explicitly designed to examine the performance of these methods when only a small number of drillholes are available. To achieve this, an initial block model was constructed using geophysical parameters (*ER* and *M*) as auxiliary variables together with assay data from five drillholes. Each technique was applied to estimate copper grade and tonnage. Subsequently, a benchmark block model was developed using assay data only from the complete dataset from twelve drillholes, and the discrepancies between the two models were used to quantify the estimation errors and evaluate methods performance.

The results show that chargeability data provide a more effective auxiliary predictor than *ER* from modelling copper mineralization in the Mesgaran VMS deposit. Although all three methods (regression, cokriging, and ANN) reproduced a similar mean grade of 0.15%, their global predictions were different. Regression analysis tended to overestimate total resource value, whereas cokriging produced systematic underestimation. The ANN delivered the closest agreement with the benchmark model, exhibiting the lowest error in tonnage and demonstrating greater ability to capture the non-linear relationship between *M* (chargeability) and copper grade.

Overall, the comparison between the five – drillhole and twelve-drillhole models confirms that ANN and cokriging are both viable for resource estimation in sparse-data setting. However ANN provides higher accuracy and operational robustness. The proposed workflow-integrating limited drilling data with geophysical surveys through ANN-offers a practical and generalizable framework for early feasibility evaluations in similar structurally complex and data-constrained exploration environments.

Funding

The authors declare that no funds, or other support were received during the preparation of this manuscript.

6. References

Azevedo, L., & Soares, A. (2017). Geostatistical methods for reservoir geophysics (p. 141). Berlin: Springer.

Babaei, M., Abedi, M., Norouzi, G. H., & Kazem Alilou, S. (2020). Geostatistical modeling of electrical resistivity tomography for imaging porphyry Cu mineralization in Takht-e-Gonbad deposit, Iran. Journal of Mining and Environment, 11(1), 143-159.

Biswas, A., & Sharma, S. P. (2016). Integrated geophysical studies to elicit the structure associated with Uranium mineralization around South Purulia Shear Zone, India: A Review. Ore Geology Reviews, 72, 1307-1326. https://doi.org/10.1016/j.oregeorev.2014.12.015

Boezio, M. N. M., Costa, J. F. C. L., & Koppe, J. C. (2011). Ordinary Cokriging of Additive Log-Ratios for Estimating Grades in Iron Ore Deposits, Proceedings of the 4th International Workshopon Compositional Data Analysis. CIMNE. Sant Feliu de Guíxols, 1-5 June, 2011

Bourges, M., Mari, J. L., & Jeannée, N. (2012). A practical review of geostatistical processing applied to geophysical data: methods and applications. Geophysical prospecting, 60(3), 400-412.

Dahlin, T., Leroux, V., & Nissen, J. (2002). Measuring techniques in induced polarisation imaging. Journal of Applied Geophysics, 50(3), 279–298. https://doi.org/10.1016/S0926-9851(02)00148-9

Dutta, S., Misra, D., Ganguli, R., Samanta, B. & Bandopadhyay, S. (2006). A hybrid ensemble model of Kriging and neural network for ore grade estimation. International Journal of Mining, Reclamation and Environment, 20(1), 33-45. https://doi.org/10.1080/13895260500322236

Embaby, A., Ismael, A., Ali, F. A., Farag, H. A., Mousa, B. G., Gomaa, S., & Elwageeh, M. (2023). An approach based on Machine Learning Algorithms, Geostatistical Technique, and GIS analysis to estimate phosphate ore grade at the Abu Tartur Mine, Western Desert, Egypt. Mining of Mineral Deposits, 17(1). https://doi.org/10.33271/mining17.01.108

Everett, M. E. (2013). Near-surface applied geophysics. Cambridge University Press. P.105

Ferdows, S.M., & Ramazi, H. (2015) Application of the fractal method to determine the membership function parameter for geoelectrical data (case study: Hamyj copper deposit, Iran). Journal of Geophysics and Engineering, 12(1), 909-921. https://doi.org/10.1088/1742-2132/12/6/909

Fink, J.B., McAlister, E.O., Sternberg, B.K., Wieduwilt, W.G., & Ward, S.H. (1990). Induced polarization, applications and case histories. Investigations in Geophysics: Society of Exploration Geophysicists. https://doi.org/10.1190/1.9781560802594

Galetakis, M. (1999). Application of Artificial Neural Networks in Solving Problems Related with Open Pit Mine Planning and Design. Mineral Wealth-Athens, 113, 47–56.

Hanifehnia, J., Esmaeilzadeh, A., Mikaeil, R., & Atalou, S. (2024). Prediction of blast-induced flyrock by using neural-imperialist competitive method (Case Study: Sungun Copper Mine). Rudarsko-geološko-naftni zbornik, 39(5), 109-120. https://doi.org/10.17794/rgn.2024.5.8

Hooshmand, A., Delghandi, M., Izadi, A., & Ahmadaali, K. (2011). Application of kriging and cokriging in spatial estimation of groundwater quality parameters. African Journal of Agricultural Research, 6(14), 3402–3408. https://doi.org/10.5897/AJAR11.027

Howarth, R. J. (2001). A History of Regression and Related Model-Fitting in the Earth Sciences (1636? -2000), Natural Resources Research. 10, 241-284. https://doi.org/10.1023/A:1013928826796

Jodeiri, B.S., Ardejani, F.D., Ramazi, H., & Moradzadeh, A. (2016) Predicting pyrite oxidation and multi-component reactive transport processes from an abandoned coal waste pile by comparing 2D numerical modeling and 3D geoelectrical inversion. International Journal of Coal Geology, 164: 13-24.https://doi.org/10.1016/j.coal.2016.03.014

Jodeiri, B.S., Ramazi, H., Faramarz, S., Ardejani, D., & Moradzadeh, A. (2014) Integrated Time-Lapse Geoelectrical–Geochemical Investigation at a Reactive Coal Washing

Waste Pile in Northeastern Iran. Mine Water and the Environment. 33, 256-265. https://doi.org/10.1007/s10230-014-0265-9

Ke, J. (2002). Neural network modeling for placer ore grade spatial variability. Ph.D. dissertation, University of Alaska, Fairbanks.

Khanlari, G. R., Heidari, M., Momeni, A. A., & Abdilor, Y. (2012). Prediction of shear strength parameters of soils using artificial neural networks and multivariate regression methods. Engineering Geology, 131–132, 11–18. http://doi.org/10.1016/j.enggeo.2011.12.006

Khesin, B., Alexeyev, V., & Eppelbaum, L. (1997). Rapid methods for interpretation of induced polarization anomalies, Journal of Applied Geophysics. 37(2), 117- 130. https://doi.org/10.1016/S0926-9851(97)00006-2

Knotters, M., Brus, D.J., & Voshaar, J.H.O. (1995). A comparison of kriging, co-kriging and kriging combined with regression for spatial interpolation of horizon depth with censored observations. Geoderma, 67(3-4), 227–246. https://doi.org/10.1016/0016-7061(95)00011-C

Koike, K., & Matsuda, S. (2003). Characterizing content distributions of impurities in a limestone mine using a feed-forward neural network. Natural resources research, 12, 209-223. https://doi.org/10.1023/A:1025180005454

Koike, K., Matsuda, S., Suzuki, T. & Ohmi, M. (2002). Neural network-based estimation of principal metal contents in the Hokuroku District, northern Japan, for Exploring Kuroko-type deposits. Natural resources research, 11, 135-156. https://doi.org/10.1023/A:1015520204066

Kumar, D., Ahmed, S., Krishnamurthy, N. S., & Dewandel, B. (2007). Reducing ambiguities in vertical electrical sounding interpretations : A geostatistical application. Journal of Applied Geophysics, 62(1) 16–32. http://doi.org/10.1016/j.jappgeo.2006.07.001

Li, X., Xie, Y., Guo, Q., & Li, L. (2010). Adaptive ore grade estimation method for the mineral deposit evaluation. Mathematical and Computer Modelling, 52(11–12), 1947–1956. http://doi.org/10.1016/j.mcm.2010.04.018.

Loke, M. H., & Barker, R. D. (1996a). Practical techniques for 3D resistivity surveys and data inversion. Geophysical Prospecting, 44(3), 499–523. https://doi.org/10.1111/j.13652478.1996.tb00162.x

Loke, M. H., & Barker, R. D. (1996b). Rapid least-squares inversion of apparent resistivity pseudosections by a quasi-Newton method. Geophysical Prospecting, 44(1), 131–152. https://doi.org/10.1111/j.1365-2478.1996.tb00142.x

Malvić, T., Ivšinović, J., Barudžija, U., Brajnović, I., & Rudec, M. (2025). Comparison of the Polynomial Regression Zonal Estimation Comparison of the Inverse Distance Weighting and Ordinary Kriging Linear Interpolator: Case Study of Porosity Estimation in Neogene Sandstone Reservoirs in the Sava Depression, Croatia. Rudarsko-geološko-naftni zbornik, 40(4), 185-196. https://doi.org/10.17794/rgn.2025.4.14

Malvić, T., Barišiæ, M., & Futiviæ, I. (2009). Cokriging geostatistical mapping and importance of quality of seismic attribute (s). Nafta, 60(5), 259-264.

Mandal, A., Biswas, A., Mittal, S., Mohanty, W. K., Sharma, S. P. Sengupta, D., Sen, J., Bhatt, A. K. (2013). Geophysical anomalies associated with uranium mineralization from Beldih mine, South Purulia Shear Zone, India. Journal Geological Society of India, 82(6), 601-606. https://doi.org/10.1007/s12594-013-0197-1

Mashhadi, S.R., Mostafaei, K., & Ramazi, H. (2017) Improving bitumen detection in resistivity surveys by using induced polarisation data. Exploration Geophysics, 49(5), 762-774. https://doi.org/10.1071/EG17032.

Misra, D., Samanta, B., Dutta, S. & Bandopadhyay, S. (2007). Evaluation of artificial neural networks and Kriging for the prediction of arsenic in Alaskan bedrock-derived stream sediments using gold concentration data. International Journal of Mining, Reclamation and Environment, 21(4), 282-294. https://doi.org/10.1080/17480930701259294

Mostafaei, K., & Ramazi, H. (2018a). Compiling and verifying 3D models of 2D induced polarization and resistivity data by geostatistical methods. Acta Geophysica, 66, 959-971.

Mostafaei, K., & Ramazi, H. (2018b). 3D model construction of induced polarization and resistivity data with quantifying uncertainties using geostatistical methods and drilling (Case study: Madan Bozorg, Iran). Journal of Mining & Environment, 9(4), 857-872. https://doi.org/10.22044/jme.2018.6852.1516

Mostafaei, K., & Ramazi, H. (2019). Mineral resource estimation using a combination of drilling and IP-Rs data using statistical and cokriging methods. Bulletin of the mineral research and exploration, 160(160), 177-195.

Mostafaei, K., Ramazi, H., & Jalali, M. (2014). Application of Integrated Geophysical and Geostatistical Methods in Amiriyeh Site Classification. Geodynamics Research International Bulletin (GRIB), 2 (2).1-15.

Mostafaei, K., Zamani, M.A.M., & Knez, D. (2022a). Risk management prediction of mining and industrial projects by support vector machine. Resources Policy, 78, 102819. https://doi.org/10.1016/j.resourpol.2022.102819

Mostafaei, K., & Kianpour, M. (2022b). Application of Magnetometry in Manto-type Copper Deposit Exploration, Case study: Meyami, Iran. Rudarsko-geološko-naftni zbornik, 37(5), 1-14. https://doi.org/10.17794/rgn.2022.5.1

Mostafaei, K., Maleki, S., Jodeiri Shokri, B., & Yousefi, M. (2023). Predicting gold grade by using support vector machine and neural network to generate an evidence layer for 3D prospectivity analysis. International Journal of Mining and Geo-Engineering, 57(4), 435-444.

Nguyen, L. Q., Le, T. T. T., Nguyen, T. G., & Tran, D. T. (2023). Prediction of underground mining-induced subsidence: Artificial neural network based approach. Mining of Mineral Deposits, 17(4), 45-52. https://doi.org/10.33271/mining17.04.045

Park, G., Oh, S., Lee, H., Kim, J. H., & Kwon, B. D. (2011). Geostatistical integration of gravity and magnetotelluric data to enhance resolution of geologic structure. Journal of applied geophysics, 73(3), 232-242.

Reynolds, J. M. (2011). An Introduction to Applied and Environmental Geophysics: John Wiley & Sons. Pp. 696.

Salarian, S., Asghari, O., Abedi, M., & Alilou, S. K. (2020). Geostatistical-based geophysical model of electrical resistivity and chargeability to image Cu mineralization in Ghalandar deposit, Iran. International Journal of Mining Geo-Engineering, 54(2), 153-160.

Salarian, S., Oskooi, B., Mostafaei, K., & Smirnov, M. Y. (2024). Improving the resource modeling results using auxiliary variables in estimation and simulation methods. Earth Science Informatics, 17(5), 4161-4181. https://doi.org/10.1007/s12145-024-01383-7

Samanta, B., Bandopadhyay, S., Ganguli, R. & Dutta, S. (2005). An application of neural networks to gold grade estimation in Nome placer deposit. Journal of South African Institute of Mining and Metallurgy. 105, 237-246.

Šapina, M. (2016). A comparison of artificial neural networks and ordinary kriging depth maps of the lower and upper Pannonian stage border in the Bjelovar Subdepression, Northern Croatia. Rudarsko-geološko-naftni zbornik, 31(3), 75-86. https://doi.org/10.17794/rgn.2016.3.6

Shademan, K.M., Madani, H., Hassani, H. O. H., & Oarefvand, P. A. M. (2013). Determining the Best Search Neighbourhood in Reserve Estimation, using Geostatistical Method: A Case Study Anomaly No 12A Iron Deposit in Central Iran. Journal of the Geological Society of India, 81(12), 581–585. https://doi.org/10.1007/s12594-013-0074-y

Singer, D.A. & Kouda, R. (1996). Application of a feedforward neural network in the search for Kuroko deposits in the Hokuroku district, Japan. Mathematical Geology, 28, 1017-1023. https://doi.org/10.1007/BF02068587

Singh, U.K., Tiwari, R.K., & Sing, S.B. (2013). Neural network modeling and prediction of resistivity structures using VES Schlumberger data over a geothermal area. Computers and Geosciences, 52, 246–257. https://doi.org/10.1016/j.cageo.2012.09.018

Stanley, S. J., & Bolton, G. T. (2008). A review of recent electrical resistance tomography (ERT) applications for wet particulate processing. Particle & Particle Systems Characterization, 25(3), 207-215. https://doi.org/10.1002/ppsc.200701126

Tutmez, B., Tercan, A. E., & Kaymak, U. (2007). Fuzzy Modeling for Reserve Estimation Based on Spatial Variability. Mathematical Geology, 39(1), 87-110. http://doi.org/10.1007/s11004-006-9066-4.

Wang, Q., Deng, J., Liu, H., Yang, L., Wan, L., & Zhang, R. (2010). Fractal models for ore reserve estimation. Ore Geology Reviews, 37(1), 2–14. http://doi.org/10.1016/j.oregeorev.2009.11.002.

White, R. M. S., Collins, S., & Loke, M. H. (2003). Resistivity and IP arrays, optimised for data collection and inversion. ASEG Extended Abstracts, 2003(2), 1-4. https://doi.org/10.1071/ASEG2003ab182

Wu, X. & Zhou, Y. (1993). Reserve estimation using neural network techniques. Computer and Geosciences, 19(4), 567 – 575. https://doi.org/10.1016/0098-3004(93)90082-G

Xu, H., Sun, J., Russell, B., & Innanen, K. (2015). Porosity prediction using cokriging with multiple secondary. CREWES Research Report, (27), 1-13

Yama, B.R. & Lineberry, G.T. (1999). Artificial neural network application for a predictive task in mining. Mining Engineering, 51(2), 59-64.

SAŽETAK

Predviđanje mineralnih rezervi kombinacijom geofizičkih i bušotinskih podataka korištenjem regresije, kokriginga i umjetne neuronske mreže u ležištu bakra Mesgaran, Iran

Tijekom studije izvedivosti rudarskoga projekta potrebno je uspostaviti prediktivni model u svrhu procjene profitabilnosti ležišta minerala. U ovome istraživanju uspostavljena su tri modela integriranjem geofizičkih podataka koji uključuju induciranu polarizaciju (IP), električnu tomografiju (ERT) i bušotinske podatke. Pri tome su korištene metode regresije, kokriginga i umjetne neuronske mreže (ANN) s ciljem utvrđivanja profitabilnosti proizvodnje minerala u ležištu bakra Mesgaran. Ležište Mesgaran nalazi se u središnjemu dijelu pokrajine Južni Horasan u Iranu. Podatci o naboju (M) i električnoj otpornosti korišteni su kao ulazni parametri, a sadržaj bakra kao izlazna varijabla. Rezultati prediktivnih modela uspoređeni su sa stvarnim modelom konstruiranim na temelju dvanaest bušotina izbušenih nakon provedbe studije izvedivosti. Na temelju provedenih analiza utvrđeno je da su podatci IP-a prikladniji od podataka električne otpornosti u svrhu izrade 3D ekonomskoga modela ležišta bakra. Osim toga, sva tri prediktivna modela procijenila su prosječni sadržaj bakra na gotovo 0,15 %. Ipak, otkrivena je znatna razlika u njihovim predviđenim vrijednostima tonaže i profita. Zaključeno je da ANN algoritam pruža točnije i pouzdanije procjene za procjenu mineralnih resursa. Rezultati ovoga istraživanja mogu se uspješno koristiti u financijskoj analizi rudarskih projekata.

Ključne riječi:
procjena rezervi, inducirana polarizacija (IP), umjetna neuronska mreža (ANN), geostatistika

Author's contribution

Kamran Mostafaei (PhD, Assistant Professor): conceptualization, data curation, investigation, formal analysis, writing – original draft and software. **Hamidreza Ramazi** (PhD, Professor): supervision, validation, review & editing. **Mohammad Zamani Ahmad Mahmoudi** (PhD): writing – review & editing. **Mitra Khalilidermani** (PhD): writing – review & editing. **Dariusz Knez** (PhD, Professor): writing – review & editing.
All authors have read and agreed to the published version of the manuscript.